Future changes in flash flood frequency and magnitude over the European Alps

Mar J. Zander[1,2], Pety J. Viguurs[3], Frederiek C. Sperna Weiland[1], and Albrecht H. Weerts[1,2]

[1]Department of Inland Water Systems, Deltares, Delft, the Netherlands
[2]Hydrology and Quantitative Water Management Group, Wageningen University and Research, Wageningen, the Netherlands
[3]TAUW Nederland, Amsterdam, the Netherlands

Correspondence: M.J. Zander (marjanne.zander@wur.nl)

Abstract. Flash Floods are damaging natural hazards which often occur in the European Alps. Precipitation patterns and intensity may change in a future climate affecting their occurrence and magnitude. For impact studies, flash floods can be difficult to simulate due the complex orography and limited extent duration of the heavy rainfall events which trigger them. The new generation convection-permitting regional climate models (CP-RCMs) improve the representation of the intensity and

5 frequency of heavy precipitation. Within CP-RCMs deep convection is resolved rather than parameterized. Therefore, this study combines such simulations with high-resolution distributed hydrological modelling to assess changes in flash flood frequency over the Alpine domain. We use output from a state-of-the-art CP-RCM to drive a high-resolution distributed hydrological wflow_sbm model covering most of the Alpine mountain range on an hourly resolution. First, the hydrological model was validated by comparing ERA5 driven simulation with streamflow observations from 130 stations (across Rhone, Rhine, Po,

10 Adige and Danube basins). Second, a hourly wflow_sbm simulation driven by a CP-RCM downscaled ERAInterim simulation was compared to databases of past flood events to evaluate if the model can accurately simulate flash floods and to determine a suitable threshold definition for flash flooding. Finally, simulations of the future climate RCP 8.5 for the end-of-century (2096-2105) and current climate (1998-2007) are compared for which the CP-RCM is driven by a Global Climate Model. The simulations are compared to assess if there are changes in flash flood frequency and magnitude using a threshold approach.

15 Results show a similar flash flood frequency for autumn in the future, but a decrease in summer. However, the future climate simulations indicate an increase in the flash flood severity in both summer and autumn leading to more severe flash flood impacts.

1 Introduction

Flash floods are sudden torrential floods, triggered by high-intensity mostly short-duration localized rainstorms (Gaume et al.,

20 2009; Amponsah et al., 2018; Kuksina et al., 2017). Flash floods have a high mortality rate compared to other flood types and lead to serious economic damage (Gaume et al., 2009; Jonkman, 2005; Marchi et al., 2010). They often occur in mountainous areas where the combination of orography triggered convection, small catchments, and steep slopes can lead to a rapid concentration of runoff (Barredo, 2007; Kuksina et al., 2017). Therefore they are a major natural hazard in the European Alps.

Observational records show increases in the intensity of extreme rainfall over the past decades, primarily for short sub-daily

25   durations (Westra et al., 2014; Förster and Thiele, 2020). This intensification is expected to become more apparent in the future

when higher temperatures lead to an increase in the moisture-holding capacity of the atmosphere (the Clausius-Clapeyron

relationship) (e.g. Lenderink and Van Meijgaard, 2008, 2010; Ban et al., 2014, 2015). According to Kotlarski et al. (2023),

who based there assessment on the CORDEX datasets, mean summer temperature rise by can reach up to 7 degrees by 2100.

Thus intensity of flash floods and thereby their impacts may increase. Therefore, there is a need to adapt, and projections of

30   future flash flood behaviour can inform adaptation strategies (Gobiet et al., 2014).

Their limited spatial and temporal extent and the relative remoteness of where they occur hampers documentation on flash

floods in mountainous areas, hindering regional studies on flash floods (Modrick and Georgakakos, 2015).

For future impact studies, high-resolution data would be needed. Recent developments have opened the door for regional-

scale flash flood modelling studies: The increasing availability of high-resolution Earth observation data enables high resolution

35   distributed hydrological modelling (e.g. Imhoff et al., 2020; Eilander et al., 2021). The publication of regional, observation-

based flood databases like Paprotny et al. (2017) and Amponsah et al. (2018) enable the validation of flash flood model results.

Furthermore, with increasing computer power, climate modellers can downscale parts of global climate models (GCMs) to

the kilometre scale: convection-permitting regional climate models (CP-RCMs). This scale increase improves the simulation

of orographic precipitation due to the higher surface resolution. It enables the explicit computation of deep convection, where

40   coarser-resolution regional climate models (RCMs) rely on parameterisation schemes for convective processes. This is a sub-

stantial source of errors and uncertainties for precipitation extremes (Prein et al., 2013, 2015; Ban et al., 2014; Lucas-Picher

et al., 2021). CP-RCMs can therefore enhance our understanding of changes in rainfall extremes as they can improve the hourly

statistics and diurnal cycle of the modelled rainfall as well as the spatial patterns of rainfall fields (e.g. Prein et al., 2013; Ban

et al., 2014; Kendon et al., 2017; Fosser et al., 2017; Ban et al., 2021; Fumière et al., 2020). See Lucas-Picher et al. (2021) for

45   a recent review.

The computational cost, runtime, and produced data volume limit the application of CP-RCMs to event-based experiments

(e.g. Hazeleger et al., 2015; Manola et al., 2017; Schaller et al., 2020; Hegdahl et al., 2020), or simulation periods of about a

decade (e.g. Leutwyler et al., 2017; Coppola et al., 2020; Ban et al., 2021; Pichelli et al., 2021).

While several hydrological modelling studies have used RCMs like the EURO-CORDEX simulations (Jacob et al., 2014)

50   for climate change impacts on flooding (e.g. Smiatek and Kunstmann, 2019; Brunner et al., 2019; Di Sante et al., 2021; Alfieri

et al., 2015), the application of CP-RCMs in hydrological studies is not common practice.

Pioneering recent work has shown that combinations of CP-RCMs and hydrological impact models can be applied to gain

new insights on local and regional changes in flood impacts with a changing climate (Kay et al., 2015; Reszler et al., 2018;

Felder et al., 2018; Rudd et al., 2020; Schaller et al., 2020). Although Kay et al. (2015) showed that finer resolution CP-

55   RCMs do not automatically lead to more reliable hydrological modelling for large-scale river flooding, they indicate that

small flashy catchments may show different results. Schaller et al. (2020) show that a model chain consisting of a CP-RCM

and a distributed hydrological model can reproduce extreme rainfall events and subsequent flooding over two of such flashy

mountainous catchments in Norway. Furthermore the authors conclude that hydrological modelling at an hourly resolution is

necessary to capture the peak streamflow due to the fast flood generating processes. Using a 'storyline approach,' the events
60   were translated into an ensemble of plausible future events taking RCP 4.5 for the end-of-century scenario. Not all modelled
events in the ensemble hit the studied catchments (Schaller et al., 2020).

Felder et al. (2018) use an event-based modelling chain with CP-RCMs, hydrological and hydraulic models, and loss mod-
elling to explore the feasibility of determining flood impacts from simulated extreme weather in a GCM to the building scale
in the Alpine Aare catchment. Their study, however, limits itself to one Alpine catchment. While Rudd et al. (2020) takes a
65   regional approach to surface water flooding in Southern England using CP-RCM simulations to drive a gridded hydrological
model. They found larger changes in precipitation than in surface runoff, indicating an added value of using hydrological
modelling over purely applying thresholds on the simulated rainfall amounts in CP-RCMs (Rudd et al., 2020).

Reszler et al. (2018) use an ensemble of two RCMs at three spatial resolutions including at convection-permitting scale (ca.
3 km) as input for distributed hydrological modelling in three catchments in the Austrian Alps. They find one of the CP-RCMs
70   outperforms other simulations on most flood statistics including the seasonality of floods. However, they conclude to finding
no clear added value of the CP-RCM simulations due to lacking realism in the temporal distribution of rainfall intensities at a
sub-daily scale and/or total precipitation amount per rainfall event (Reszler et al., 2018).

In this research, we take a regional approach to simulating flash floods in the European Alps using ten-year transient CP-
RCM simulations and high-resolution hydrological modelling (1km). The regional approach allows for using the high spatial
75   resolution of the climate simulation data. We aim to validate the ability of the CP-RCM - hydrological model combination to
simulate flash floods and assess changes in their frequency and magnitude for the current and future climate. The hypothesis
is that by using a form of trading space for time, given the relatively short simulation periods of 10 years available and using
a large enough spatial domain, we can assess future flash flood frequency and magnitude changes over the European Alpine
domain. For the hydrological modelling, we use the wflow_sbm model that is able to simulate with short time steps and at
80   a high spatial resolution and relatively large spatial domains, and which was used previously to model the Rhine including
part of the Alps (Imhoff et al., 2020). Wflow_sbm simulates all processes important for flash flooding (e.g. Infiltration excess,
saturation excess, Hortonian overland flow, see van Verseveld et al. (2022)). The transient periods ensure that hydrological
processes and conditions important to flash flood development, such as initial soil moisture content, are considered.

2   Data and Method

2.1   Study Area

The European Alps are a mountain range of 800 kilometres long and have an average width of 200 kilometres (Schär et al.,
1998). The ridge height is about 2.5 kilometres. The European Alps are characterised by deeply incised valleys and extensive
lowlands and have considerable topographic variability (Gobiet et al., 2014). The study area covers most of the European Alpine
mountain range encompassing many river basins; the Upper Rhone river until Geneva, the High Rhine & Alp Rhine until Basel,
90   Adige to just South of Trento, and the Alpine tributaries to the Danube, Alpine part of the tributaries to the Po basin. The study
domain falls within Italy, Switzerland, Liechtenstein, Austria, and France. The modelled domain contains many glaciers, lakes,
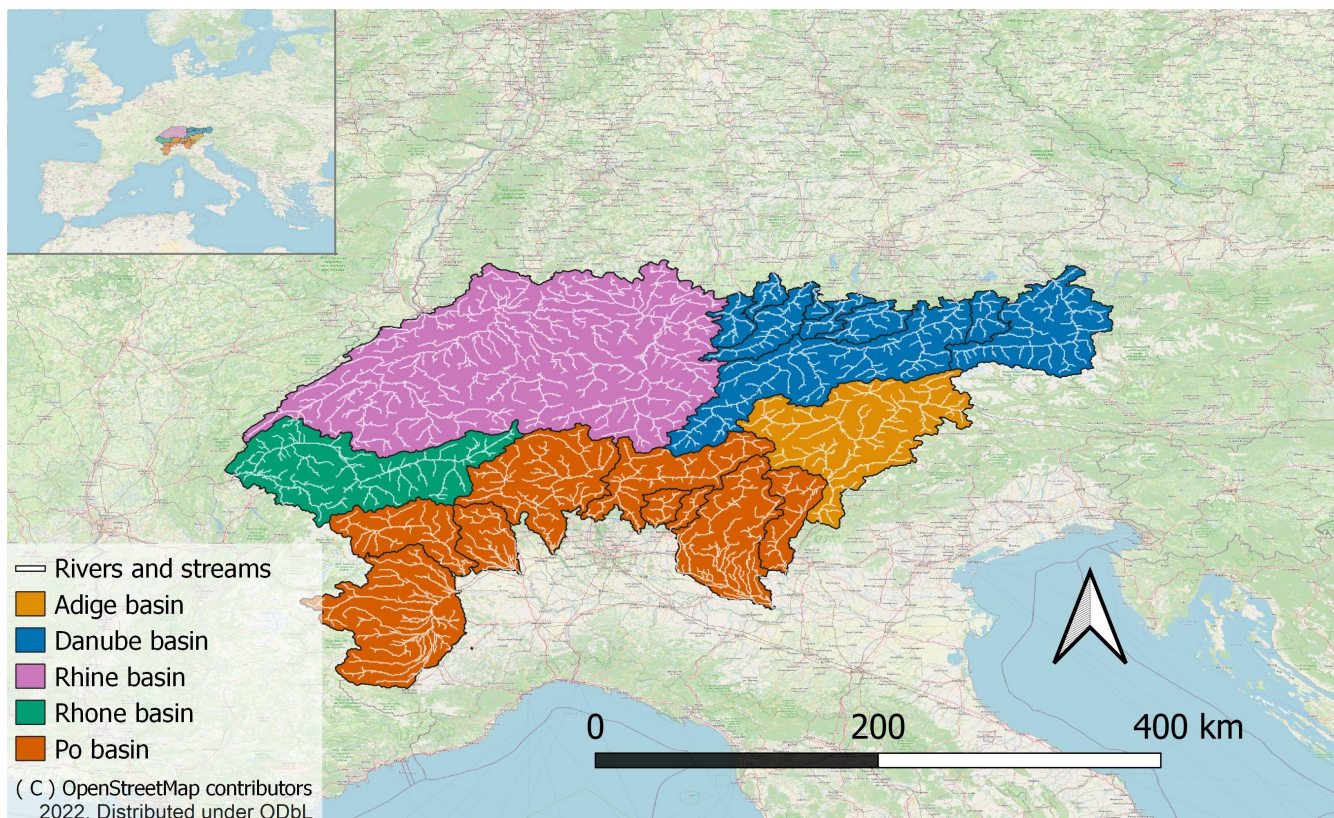
Figure 1. Hydrological modelling domain over the European Alps with the basins and tributaries to the Adige (yellow), Danube (blue), Po (orange), Rhine (pink) and Rhone (green), background map © OpenStreetMap contributors (2017).

hydropower dams and reservoirs. See Figure 1 for an overview of the domain. The annual precipitation is around 1400-1500 mm/year, with more precipitation in the West and South (Quaile, 2001). The Alpine rivers have snow and glacier melt regimes with peak discharges in late spring and early summer (May, June, July) and low discharges in winter (Meile et al., 2011). Most

95 flash floods in the European Alps occur in late summer and autumn (Gaume et al., 2009; Froidevaux et al., 2015). In France and Italy, flash floods occur primarily in autumn (September, October, November), while in Austria, most flash floods occur in late summer (August, September) (Gaume et al., 2009). For Switzerland, summer is the most important season for floods including flash floods (Froidevaux et al., 2015). The high surface temperature of the Mediterranean Sea in late summer and autumn can load the atmosphere with large amounts of water vapour. Such loaded conditionally unstable air masses advect

100 to the coast, where the relief channels them and forces them to lift. This can lead to intense convective rainfall events, which cause flash floods (Doswell et al., 1996; Tarolli et al., 2012).

Hydrology and
Earth System
Sciences
Discussions

Open Access

EGU

2.2   Convection Permitting Regional Climate Model

The convection-permitting climate model used is the Unified Model, MetOffice Hadley Center UKMO 2.2 km (UM version 10.1) as described by Berthou et al. (2018). In a recent CP-RCM intercomparison study, this model performed well in terms of simulated precipitation over the Alps (Ban et al., 2021). Modelled precipitation is available as hourly sums, along with three-hourly near-surface air temperature, six-hourly surface pressure, and daily mean incoming solar shortwave radiation at the surface.

Three UM simulations are used: a reference UM simulation driven by Era-Interim reanalysis data as lateral boundary conditions (Dee et al., 2011) from 2000 to 2012, from hereon the 'Evaluation' simulation. And two climate simulations which are directly driven by the HadGEM3-GC3.1-N512 GCM and use a 360-day calendar (Williams et al., 2018). The current climate is simulated for the period of 1998-2007, referred to as the 'Historical Climate' simulation, and for the future climate change scenario RCP 8.5 van Vuuren et al. (2011) is used to simulate the period 2096 - 2105, from hereon 'Future Climate' (see Table 1). The Evaluation simulation serves to assess the quality of the model, while the GCM-driven Historical Climate and Future Climate simulations serve to assess the differences that could be attributed to climate change.

2.2.1   Climate Model Data Processing

. Ban et al. (2021), compare a set of RCMs and CP-RCMs including the UM. The comparison shows that biases in simulated precipitation statistics (99 percentile, frequency and intensity of extremes) compared to observed statistics are very small (less than 5 percent) for winter in spring for the UM. Biases are larger in summer and autumn (-5 to -25 percent). Yet, also for these seasons the UM model is one of the best performing models. Overall, the CP-RCMs outperform the RCMs. Chan et al. (2020) analyzed the projections in precipitation extremes for these datasets. Their results show that current extreme hourly events (1/yr) will in the future occur more often over the Alps. They also differentiate between winter and summer season. In winter the model projects an increase of these extreme hourly events, while for summer a decrease is projected. For daily extremes there is no clear change signal. From the wflow model input we see that annual mean discharge is projected to decrease for all basins. Decreases are largest (300 mm) for the Rhone, Adige and Western part of the Danube basin.The climate model data is remapped from its rotated pole grid to WGS84 coordinates, remapping the precipitation conservatively. We remap all fields to the resolution of the hydrological model grid. We linearly interpolate the surface level pressure and temperature to hourly values. Because remapping daily mean radiation to an hourly sinusoidal solar radiation pattern is not unambiguous, we chose to assign a uniform radiation flux to each hour of the day corresponding to the modelled average. We expect this has minimal impact on the model outcomes; see also van Osnabrugge et al. (2019). From the temperature, pressure and radiation fields, the potential evapotranspiration is calculated using the formulation of de Bruin et al. (2016).

2.3   Hydrological Model

In this study, we use the wflow_sbm hydrological model (Schellekens et al., 2021; Imhoff et al., 2020), it is a spatially distributed bucket-style model. It uses the kinematic wave routing for surface, channel and lateral subsurface flow. The wflow_sbm

is developed to maximise the use of high-resolution spatial data from Earth observations. The wflow_sbm model simulates pro-

135 cesses that are important for flash flooding (e.g. Infiltration excess, saturation excess, Hortonian overland flow, see Verseveld et al (2022)) and can run at high temporal and spatial resolution for relatively large spatial domains Models can be set up for river basins around the globe using open data at various spatial resolutions (Eilander et al., 2023). The model parameters are estimated from point-scale (pedo)transfer functions (Imhoff et al., 2020; van Verseveld et al., 2022; Sperna Weiland et al., 2021).

140 For this study, the domain is divided into seven submodels of 5 Alpine basins to improve computation times (Adige, Danube, Po, Rhine and Rhone, see Figure 1). All models of the study domain are set up in the same manner with 0.008333-degree cell sizes, corresponding to roughly one kilometre. The river network is derived using the method of Eilander et al. (2021). In addition, we use the same a priori parameter estimation methodology as Imhoff et al. (2020).

We take the Hydro-MERIT high-resolution raster hydrography maps as the base for the modelling (Yamazaki et al., 2019).

145 For the lakes, we use hydroLAKES (Messager et al., 2016), taking the minimum lake area to consider $1 km^2$, we take reservoirs from the GRanD database likewise taking the minimum area to consider $1.0 km^2$ (Lehner et al., 2011). We use monthly MODIS leaf area index for the vegetation and land use cover from CORINE (Myneni et al., 2015).

The Alpine glaciers are schematized using the Randolph Glacier Inventory dataset (Global Land Ice Measurements from Space (GLIMS), 2017), taking the minimum modelled glacier area to consider $0.1 km^2$. Glaciers are modelled with the two

150 main processes: glacier build-up from the conversion from snow to ice, and glacier and snowmelt using a degree-day model (Imhoff et al. (2020); van Verseveld et al. (2022)). We take the same initial glacier extents and volumes for each of the wflow_sbm simulations, so no scenario of glacier disappearances is considered (e.g. projected end-of-century volume loss of up to 98.8 % for RCP 8.5 in Zekollari et al. (2019)). To test the sensitivity of our results to initial glacier extents and volumes, we simulate the Future Climate scenario for the Rhone catchment, the most glaciated of the modelled catchments, with and

155 without glaciers at the simulation start. No differences were found in the modelled flash flood occurrence and magnitude between the two simulations (see Appendix B, Figure A1).

In wflow_sbm, the horizontal saturated hydraulic conductivity can be derived from the vertical hydraulic conductivity parameter using a similar approach as Bell et al. (2007). We use a constant multiplication factor of 100 for the whole modelled domain. In other studies, this factor was to be one of the most sensitive model parameters for the wflow_sbm model (Imhoff

160 et al., 2020). Therefore, we performed a sensitivity analysis for the Alpine Rhine basin using ERA5 as forcing, in which this factor is varied from 5, 20, 50, 100, 200 & 500 [-]. The model performance is assessed for the observed discharge in the Rhine River at Basel and in the Thur River station at Andelfingen. We found that a factor of 100 was satisfactory, which is lower than the factor of 250 applied in Imhoff et al. (2020) for the entire Rhine basin up to the Netherlands. While the results were not very sensitive to the applied factor, the factor of 100 does show better performance for the Alpine Rhine at Basel and Thur (See

165 Appendix A1, Table A1). For a more detailed overview of the wflow_sbm model setup, we refer to Imhoff et al. (2020).

2.4   ERA5 Validation simulation

First we force the wflow_sbm models with daily ERA5 reanalysis data (Hersbach et al., 2018) downscaled to the hydrological model resolution and applying lapse rate correction using the DEM at the same time, in order to assess the hydrological models' ability to simulate Alpine river discharges (Validation simulation, Table 1). We validate the modelled discharge against

170   streamflow observations from a total of 130 gauging stations. Six discharge timeseries are obtained from the Global Runoff Data Centre, seven from the Provincia Autonoma di Trento, 25 from the Bundesamt für Umwelt, and 92 from the LamaH dataset (Global Runoff Data Centre , 2021; Bundesamt für Umwelt, 2021; Dipartimento Protezione Civile, Provincia Autonoma di Trento, Trento, 2019; Klingler et al., 2021). These discharge time-series are not spread evenly over the study area, with more stations available in the Danube and Rhine basins than in the Southern and Western parts with the Rhone and Po basins. To

175   assess the model performance, we calculate the Kling-Gupta Efficiency scores (KGE) (Gupta et al., 2009). As the temporal resolution of the observed discharge time-series differs, the KGE scores are calculated for mean daily discharges to make them comparable.

2.5   ERA-Interim Evaluation simulation

Next, we force the wflow_sbm models with the downscaled UM Era-Interim simulation data (Evaluation simulation, Table 1).

180   Doing so enables an assessment of the ability of the UM CP-RCM to simulate the synoptic situations leading to flash floods. We calculate the KGE scores for the same period of 2002 to 2012 for daily discharge values for the 130 gauging stations.

2.6   Flash flood validation

We use the HANZE database of damaging European Floods (Paprotny et al., 2017), and EuroMedeFF database of flash floods (Amponsah et al., 2018) to evaluate the ability of the climate and hydrological modelling chain to simulate flash floods.

185   According to these datasets, nine flash floods took place within the study domain during the 2002 - 2012 period, see Table 2 (Amponsah et al., 2018; Paprotny et al., 2017). Apart from the location, Amponsah et al. (2018) also lists the estimated peak specific discharge of the flash flood events.

To determine what will be considered a flash flood in our study, we use an adapted version of the definition of Amponsah et al. (2018):

190   – the affected catchment has a maximal size of $3000km^2$

– the peak specific discharge is at least $0.5m^3s^{-1}km^{-2}$

Here the peak specific discharge is calculated by dividing the peak discharge by the upstream catchment area (Marchi et al., 2010). In this study, we first reduce the hourly data to daily time-series by taking the maximum hourly discharge of the day. These daily maximal hourly specific discharges are than compared to the threshold value for the dates at which a flash flood

195   happened. It is a well-known issue that internal variability in a climate model can cause rainfall events to be simulated at a different location and/or time compared to the driving data (e.g. Reszler et al., 2018; Schaller et al., 2020). Furthermore, the

Table 1. Wflow_sbm Model simulations

Simulation	Driving Data	Time Period	Spatial Resolution	Temporal Resolution
Validation	ERA-5	01/01/1979 - 31/12/2019	$0.25°$	daily
Evaluation	UM - ERA-Interim	01/01/2000 – 31/12/2012	$2.2km$	hourly
Historical Climate	UM- HadGEM3-GC3.1-N512	01/01/1998 – 31/12/2007	$2.2km$	hourly
Future Climate	UM-HadGEM3-GC3.1-N512 RCP8.5	01/01/2096 – 31/12/2105	$2.2km$	hourly

HanzeFloodlist provides information on the flood location at the level of municipalities, the European NUTS3 level. To take these two things into account, we take a regional approach to the flash flood validation. We consider it a validated flood event in the hydrological simulation if an event fitting the above mentioned criteria occurs within the adjacent subcatchment of the reported flash flood within three days of the reported date.

As additional validation step, we will compare observed specific discharge and calculate a confusion matrix for each observation station and each simulation for the flash flood threshold. From these confusion matrices we calculated the F1 score and the Peirce Skill Score. In the Peirce skill score the penalty for a Type 2 error, false negative, erroneous simulation of non-occurrence, is penalised more heavily than a Type 1 error, false positive, the unfulfilled simulations of occurrence. This makes it a suitable measure of rare extreme events, such as flash floods. The F1 score on the other hand, is a balance between the precision (number of correctly simulated threshold exceedances out of all simulated threshold exceedances) and recall (number of correctly simulated threshold exceedances out of all actual observed threshold exceedances) and places a similar cost for both Type 1 and Type 2 errors. This additional analysis does penalize deviations in the modelled location of precipitation events (and resulting simulated flash floods) in contrast to the regional approach mentioned above.

2.7 Comparison Current and Future flash flood occurrence

In order to assess potential changes in flash flood occurrence between the current and future climate scenario, we force the wflow_sbm models with GCM-driven CP-RCM simulations for 1998-2007 and 2096-2105 (Table 1) and compare them. For the Future and Historical Climate simulations the specific discharge is calculated from the daily maximal discharge and upstream area for the summer (JJA) and autumn (SON) period, taking the first year of simulation as warm-up. The peak specific discharge threshold and maximal upstream area threshold are applied. We compare the frequency of threshold exceedances and the flood peak magnitudes (specific discharges) for the two simulations. Similar to Alfieri et al. (2015) we compare the two simulations after aggregation to the subbasin level as well as for the entire modelled domain (Adige, Danube, Po, Rhine and Rhone, see Figure 1)

3 Results

3.1 ERA5 Validation simulation

As can be seen in Figure 3, the hydrological model can simulate the annual cycle of discharge with low flows in winter and snowmelt, leading to discharge peaks from May to July. For most stations the KGE score ranges from $0.4 - 0.7$ (Figure 2), with a maximum of 0.82 for the Felsenbach and Vent stations. The model shows performance at the Rhine at Basel of $KGE = 0.73$, and the Adige at Trento, $KGE = 0.56$, stations near their respective catchment outlets. There are no clear spatial patterns in the model performance (Figure 2) and no dependency on station elevation or Strahler stream order (not shown). Some modelled headwaters have high KGE scores, like the Vermigliana in the Adige catchment ($KGE = 0.80$) and the Thur at Andelfingen ($KGE = 0.75$, Figure 3), while other headwater stations perform poorly. The latter is due to hydropower reservoirs and lakes which are not included in the hydrological model due to their limited size ($< 1km^2$). At both Klaushof station and Sausteinaste station, there are hydropower reservoirs upstream, which are not simulated, leading to very high overestimations of the stream-flow ($KGE = -4.53, \beta = 5.8 \& KGE = -5.98, \beta = 5.3$ respectively). For the station at Galtür, Au Trisanna, two upstream lakes are also not modelled, leading to large overestimations ($KGE = -1.07, \beta = 2.4$).
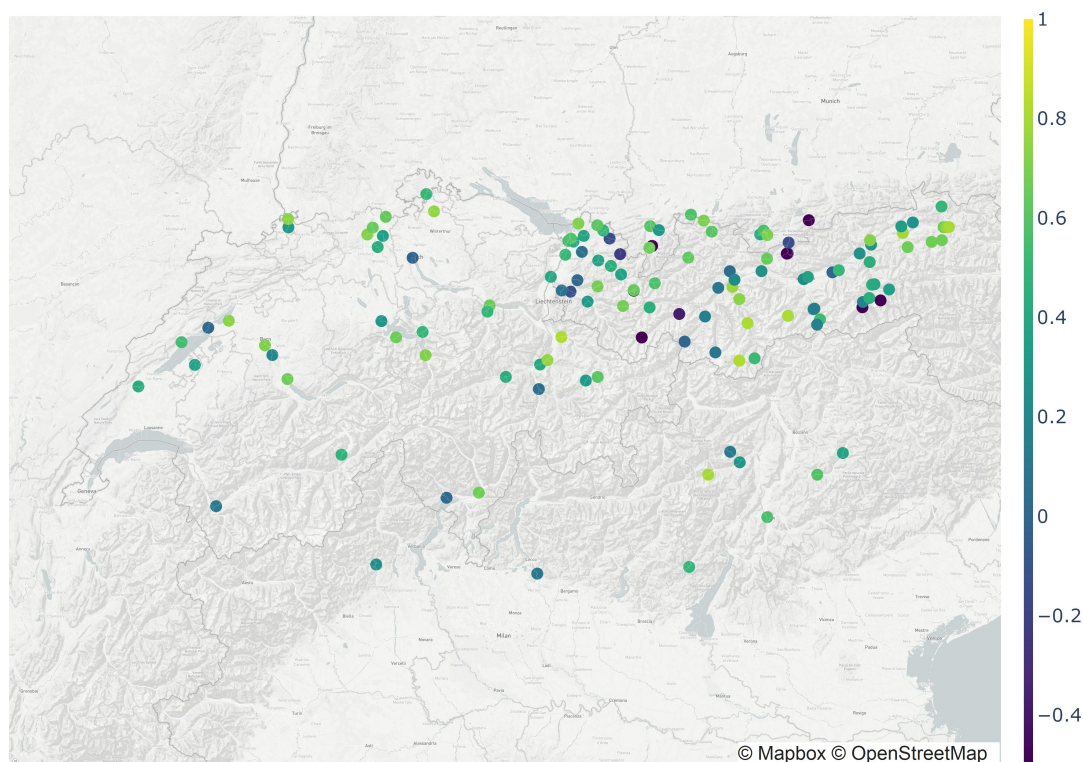

Figure 2. Map of the Kling-Gupta Efficiency score [-] for the 130 observation stations for daily discharges for 2002-2012 for the ERA5 Validation simulation.
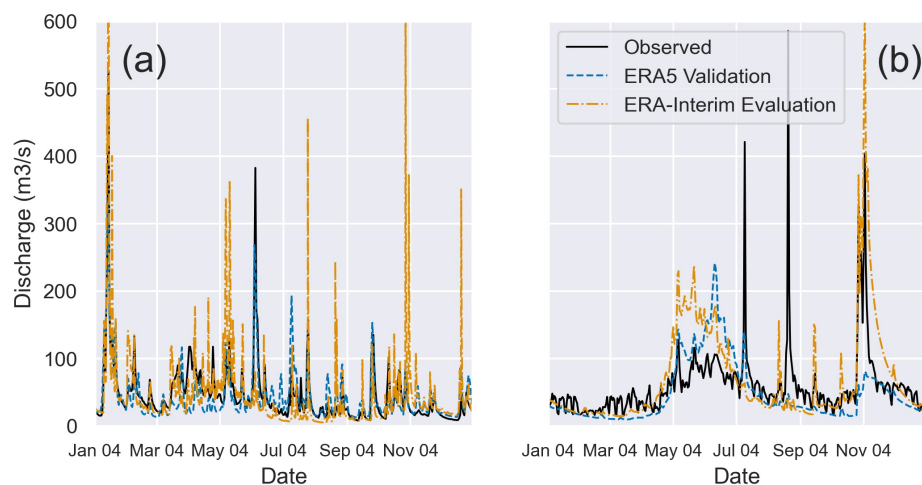
Figure 3. Observed discharge (black) compared to modelled discharges for the Validation ERA5 driven (blue) & Historical ERA-Interim driven (orange) simulations for the year 2004 for (a) Thur, Andelfingen station (Validation $KGE = 0.75$, Evaluation $KGE = 0.57$), and (b) Ticino, Bellinzona station (Validation $KGE = 0.67$, Evaluation $KGE = 0.21$).

3.2 ERA-Interim Evaluation simulation

For most stations, the ERA-Interim Evaluation UM driven simulation is in reasonable agreement with observations (Figure 3 & Figure 4). However, the ERA-5 driven Validation simulation generally outperforms the Evaluation simulation, as can be
235 seen in the histogram of station performance in Figure 4a. As can be seen from the quantile-quantile plot in Figure 4b, the difference in performance increases for stations where the simulations perform poorer.

3.3 Flash Flood Validation

Table 2 lists the nine recorded flash floods in the study area from 2002 to 2012. For all recorded flash floods, the modelled peak daily discharge was heightened compared to the preceding and following days. The modelled peak specific discharge ranged
240 from 0.47 to 2.4 $m^3s^{-1}km^{-2}$ for the documented events. For the seven riverine flood events in the model area, the modelled peaks in specific discharge were notably higher than those modelled for the inundations classified as flash floods by Paprotny et al. (2017): ranging from 1 to 4.2 $m^3s^{-1}km^{-2}$ (not shown). For the flash floods, the modelled peak specific discharges were all below the estimated ranges reported in Amponsah et al. (2018). We therefore deem the threshold of $0.5m^3s^{-1}km^{-2}$ suggested by Amponsah et al. (2018) as suitable.
245   Over the full Alpine region considered, we have thirty-four observation stations with upstream catchments of < 3000km2 with days on which the threshold of 0.5m3s-1km-2 was reached during the 2001-2009 study period. For these stations we evaluate the Peirce and F1 skill sccores. Each dot in Figure 5 represents the skill score for a single station. For those stations with
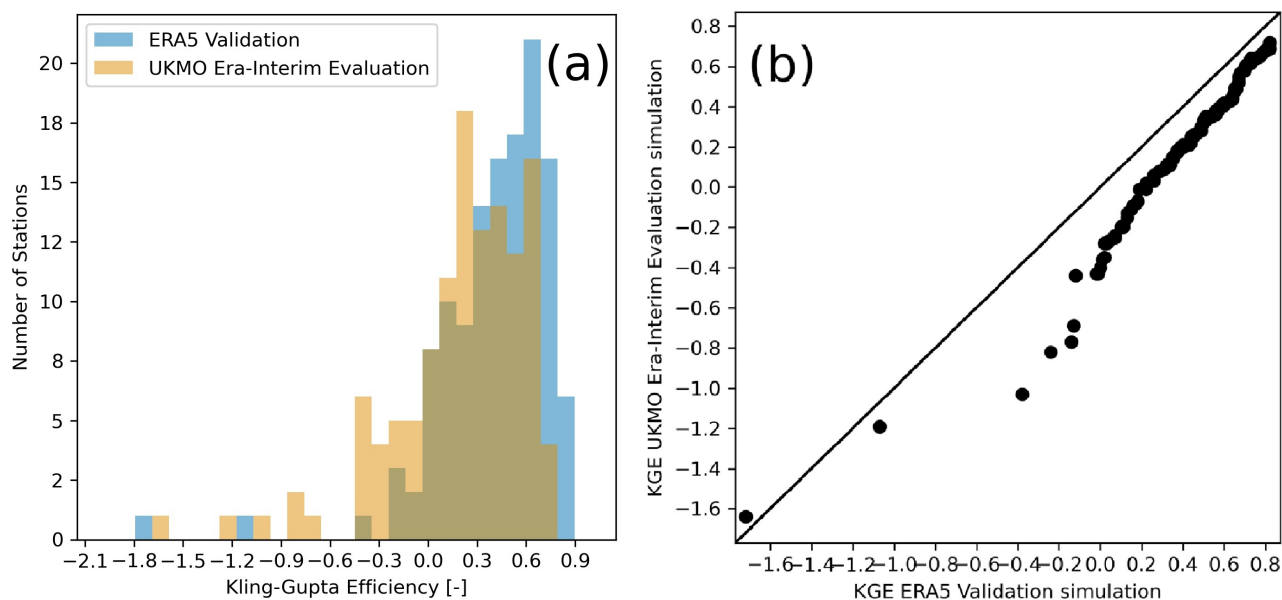
Figure 4. (a) Histograms and (b) Quantile-Quantile plot comparing the Kling Gupta Efficieny scores (KGE) [-] for the Validation ERA5 and ERA-Interim Evaluation simulations for the 130 stations.

a skill score of zero (none of) the threshold exceedances was simulated correctly. For about 1/3 of the stations the combination of UM and wflow does manage to simulate part of the threshold exceedance occurrence correctly. For 4 out of 34 stations
250 the performance is good, skill scores of 0.5 or higher. The limited performance can have several causes. The location of the precipitation event may be shifted or the intensity underestimated in the meteorological forcing. The initial conditions of the hydrological model may have been too dry, leading to a larger reduction of the runoff through infiltration.

3.4 Changes in Flash Flood Frequency and Magnitude

Figure 6 shows the cumulative distributions per modelled cell of the number of days on which the peak specific discharge ex-
255 ceeded the threshold of $0.5 m^3 s^{-1} km^{-2}$, from hereon threshold exceedances, for the Future and Historical Climate simulations and the summer and autumn seasons. Over the modelled domain, the summers have more threshold exceedances than autumns in both Historical Climate and Future Climate simulations. In summer, there are more days with threshold exceedances in the Historical Climate scenario (Figure 6). At the same time, in autumn, we see hardly any difference between the number of days with threshold exceedances in the Future Climate scenario. However, there are some regional differences. The Future Climate
260 autumn has more threshold exceedances than the Historical Climate for the Adige catchment. The seasonal differences and differences amongst the scenarios are small for the Alpine parts of the Po basin. While for the Rhine, the Historical Climate summer period has more threshold exceedances than the other periods which is in line with the changes in extreme hourly
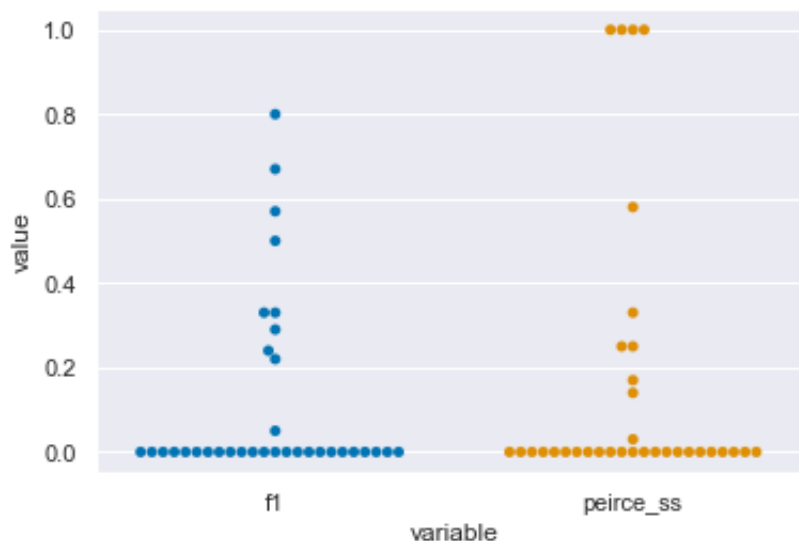
11

Figure 5. F1 skill score (left) and Peirce skill score (right) for the simulation of the 0.5m3s-1km-2 threshold exceedances for the stations with upstream areas of <3000km2

Table 2. Recorded flash floods and simulated peak specific discharges in the ERA-Interim Evaluation driven simulation, using the EuroMed-eFF (Amponsah et al., 2018) and Hanze (Paprotny et al., 2017) flood databases.

Start Recorded Date	Regions & Rivers	Modelled Peak Spec. Discharge	Date Peak Spec. Discharge	Source
5-6-2002	Sesia (Po)	1.18	5-6-2002	EuroMedeFF
6-6-2002	Rhone	1.22	5-6-2002	Hanze
6-6-2002	Danube, Rhine	2.18	6-6-2002	Hanze
8-9-2002	Rhone	0.48	9-9-2002	Hanze
24-3-2005	Rhine	0.47	24-3-2005	Hanze
3-10-2006	Isarco, Passirio (Adige)	0.49	3-10-2006	EuroMedeFF
8-6-2007	Zürich (Rhine)	2.39	7-6-2007	Hanze
12-7-2008	Po	1.35	9-7-2008	Hanze
4-8-2012	Vizze (Adige)	0.66	6-8-2012	EuroMedeFF

precipitation events found by Chan et al. (2020). Summers have more threshold exceedances than autumns for the Danube basin but with slight differences between the two scenarios.

265   Figure 7 shows box-and-whisker plots of the magnitude of the daily maximal peak specific discharges for each of the threshold exceedances. Over the entire Alpine domain, both the Future Climate summer and autumn have a higher 75 and 97.5th percentile of threshold exceedances, while the median magnitude is similar. The largest difference is in the maximal
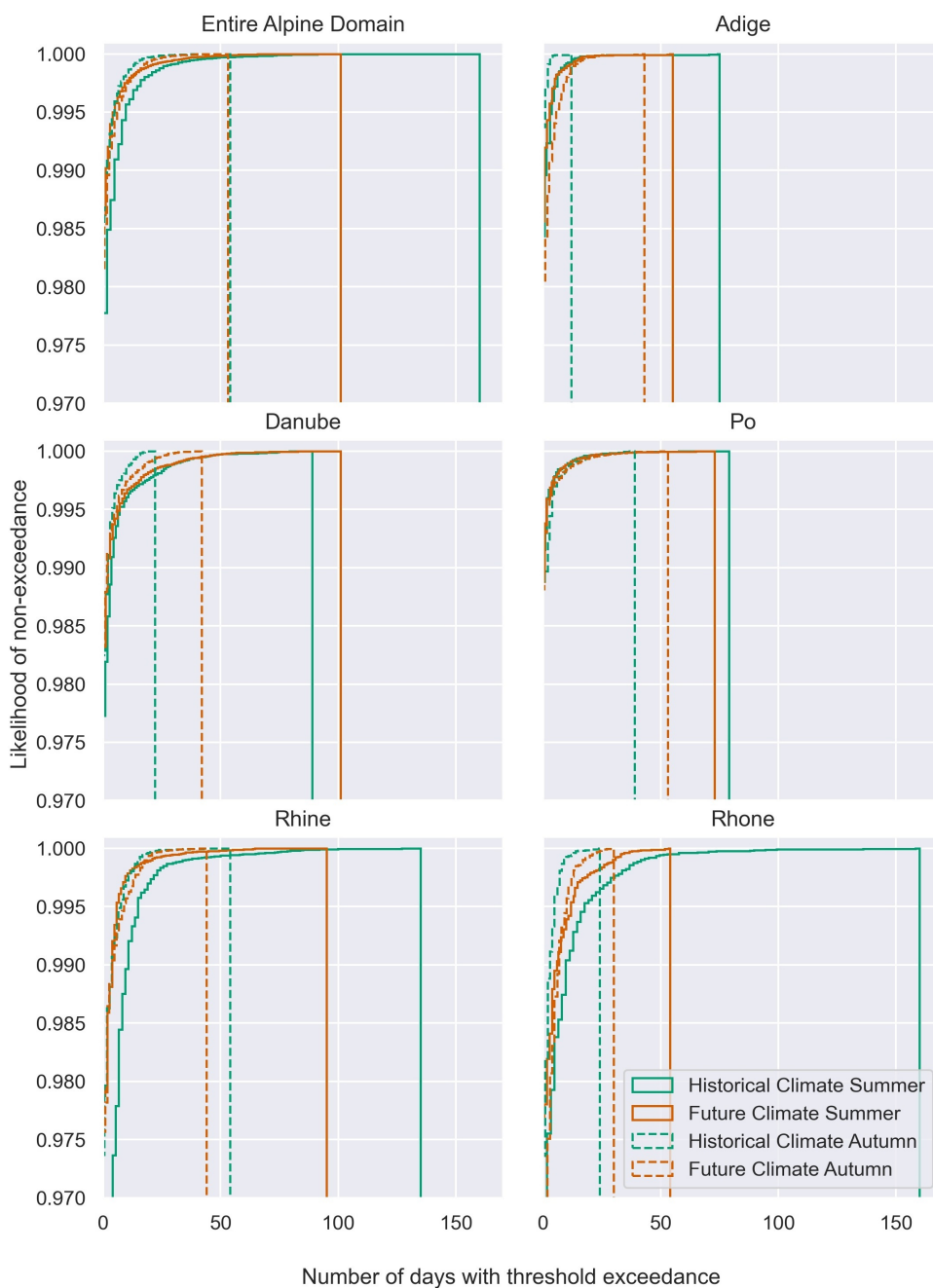
Figure 6. Cumulative distribution of the number of days on which the threshold of $0.5 m^3 s^{-1} km^{-2}$ peak specific discharge is reached over the modelled domain in summer (JJA, solid lines) and autumn (SON, dashed lines) for the Current Climate (green) and Future Climate simulation (orange). The subpanels show the entire Alpine domain, Adige, Danube, Po, Rhine and Rhone basins (see Figure 1).
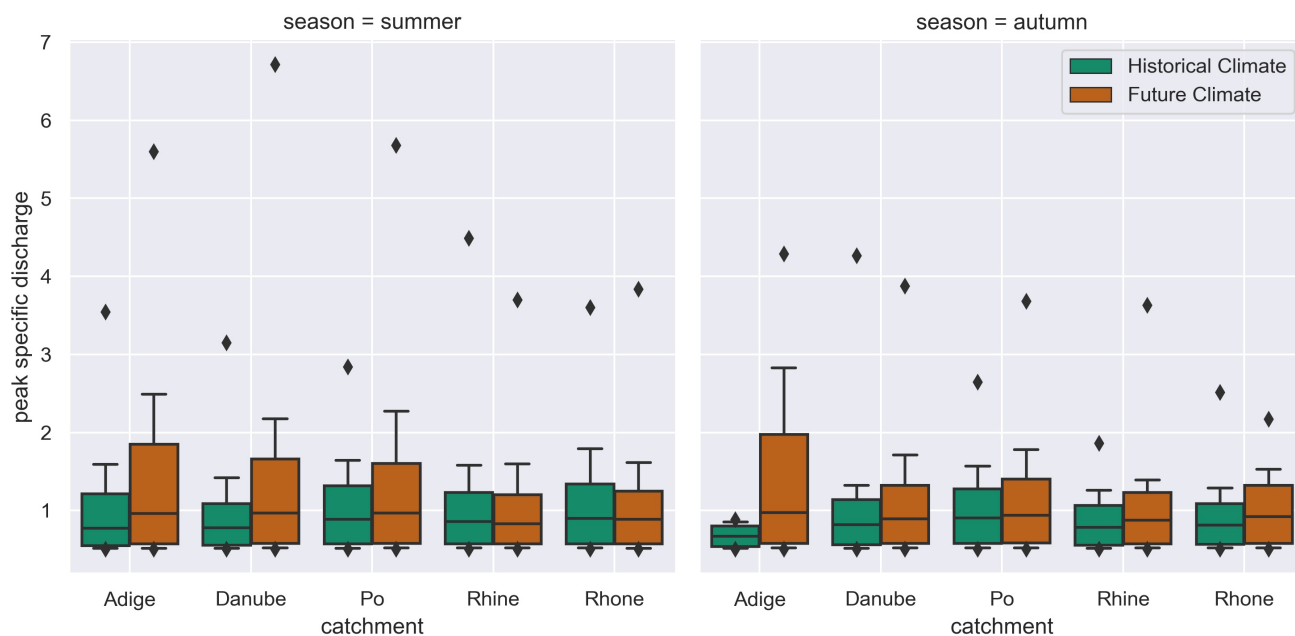
Hydrology and
Earth System
Sciences
Discussions

Open Access

EGU

Figure 7. Box-and-whisker plots for maximal daily specific discharge exceeding the 0.5 $m^3 s^{-1} km^{-2}$ specific threshold for summer (JJA) and autumn (SON) for the Historical Climate and Future Climate simulation. The boxplots show the 25th, 50th & 75th percentile, with whiskers for the 2.5^{th} & 97.5^{th} percentile and diamonds for the maximal value.

value in summer: $5.6 m^3 s^{-1} km^{-2}$ compared to $4.49 m^3 s^{-1} km^{-2}$ for the Historical Climate simulation. The maximal peak specific discharge is the same in autumn for the two Climate simulations (4.26 vs 4.29). The difference between the two

270 simulations is largest for the Adige basin, where the 50th 75, 97.5 and maximal values are higher in the Future Climate in both summer and autumn. In autumn the difference in maximal modelled specific discharge is $0.88 m^3 s^{-1} km^{-2}$ compared to $4.28 m^3 s^{-1} km^{-2}$ – a near fivefold increase.

In autumn, there are hardly any differences in the number of flash floods over the entire Alpine domain between the Current and Future Climate. However, some basins will have threshold exceedances with much higher magnitudes (Adige, Po, Rhine),

275 while others show similar maximum magnitude (Danube, Rhone).

The simulated decrease in future flash flood occurrence is most likely due to projected drying of the region, with higher temperatures, potential evaporation, and projected decreases in mean precipitation Gobiet et al. (2014); Ban et al. (2015). The antecedent soil moisture can play a significant role in the catchment response to extreme rainfall (Gaume et al., 2009). These effects will be less strong in autumn. We explicitly account for these effects by simulating these hydrological conditions over

280 the ten-year time slices.

4   Discussion on the methodology

Periods of 10 years are used in this study, as the CP-RCM model calculation time, data storage, and network requirements inhibit using longer periods (Prein et al., 2015). With such time slices, it is possible to move beyond event-based climate impact studies (e.g. Felder et al., 2018; Schaller et al., 2020). However, deriving local statistics of change is hampered. Similar

285 to Alfieri et al. (2015) and Rudd et al. (2020), the study presented here, therefore, takes a regional approach, aggregating results over larger regions. Just as in Rudd et al. (2020) we do not attempt to estimate return periods of extreme events as the simulation periods are too short to warrant such an approach. Recently, alternative statistical methods such as 'metastatistical extreme value analysis' have been applied to derive extreme value statistics from shorter time series (e.g. Marani and Ignaccolo, 2015; Zorzetto et al., 2016; Marra et al., 2018). However, these methods are applied to rainfall extremes and not the subsequent

290 hydrological response (e.g. Li et al., 2017).

For both climate and hydrological modelling, we only consider changes due to a different radiation balance by using scenario RCP 8.5. All simulations use the same initial conditions for the landscape characteristics in the hydrological model. We do not consider any scenarios of 21st-century land-use changes or plant adaptation to changes in CO_2 concentration. This limitation is familiar to many hydrological climate change impact studies (e.g. Alfieri et al., 2015; Brunner et al., 2019).

295 The CP-RCM both in the GCM driven and ERA-interim driven simulations contain biases. For instance, the UM has a wet bias in daily mean precipitation above 800 m elevation (Berthou et al., 2018; Ban et al., 2021). It was explicitly chosen not to apply a bias correction, downscaling, or a delta change approach to the climate model data as these techniques can disturb the change signal (Hagemann et al., 2011; Themeßl et al., 2012; Cloke et al., 2013; Reszler et al., 2018). Additionally, no homogeneous datasets exist for bias correction for the entire modelled Alpine domain at the resolution and time-step of the

300 CP-RCM data (Ban et al., 2021). By remapping ('downscaling') the climate data to the model resolution, we maintain the spatial coherence of the modelled precipitation and temperature fields. Furthermore, because we directly compare the two GCM driven climate simulations and thus focus on relative changes, the importance of biases for quantifying changes in flash flood frequency and magnitude is lessened.

The hydrological simulation which directly uses ERA5 reanalysis data outperforms the simulation which uses the ERA-

305 Interim UM CPM data as lateral boundary forcing (see section 3.2). This can be attributed to both the quality improvement from the Era-Interim to the ERA5 reanalysis product as well as the internal variability introduced to the CP-RCM simulation by only forcing it at the boundaries (Hersbach et al., 2018; Nogueira, 2020; Lavin-Gullon et al., 2021). The ERA 5 reanalysis dataset was, however not yet available when the UM modelling experiment was set up. Therefore, we expect more minor differences in the model performance (here KGE) for a UM simulation using ERA5 as boundary conditions and a good

310 agreement with observed discharges.

5   Conclusions and Outlook

This study presents a first regional modelling approach to studying future changes in flash flood occurrence and magnitudes. It uses a single high-resolution convection-permitting regional climate model as input for a distributed high-resolution hydro-

Hydrology and
Earth System
Sciences
Open Access
Discussions
EGU

logical model. Other studies have focused on either smaller catchments (e.g. Felder et al., 2018; Reszler et al., 2018; Schaller

315 et al., 2020), only considered surface water flooding (Rudd et al., 2020), or only focussed on riverine flooding using coarser

resolution climate simulation data for flood changes studies (e.g. Smiatek and Kunstmann, 2019; Brunner et al., 2019; Di Sante

et al., 2021; Alfieri et al., 2015).

The wflow_sbm model shows satisfactory performance, and the modelling chain of CP-RCM and distributed hydrological

modelling can reproduce recorded flash floods in the 2002-2012 period. Similar to the work of Rudd et al. (2020), we show

320 added benefit of using the combination of convection-permitting climate model and hydrological modelling as changes in

precipitation do not translate one-on-one into changes in flash floods.

Using CP-RCM simulations driven by a GCM of the Historical Climate and the end-of-century RCP 8.5 scenario as input

to the distributed hydrological modelling, the frequency of occurrence and the magnitude of the specific peak discharge are

compared. The frequency of flash floods stays the same in autumn, with more severe extremes in some basins. In summer,

325 we find a decrease in the frequency of flash floods, but with more severe extremes. This difference in maximal peak specific

discharge is most distinct in summer, where the highest simulated peak discharges are higher in the future for all basins except

the Rhine. The Adige catchment shows the largest difference in simulated flash flood magnitudes between the Future and

Historical Climate.

Assuming a relation between the flood peak and the flood impacts, we speculate that although the number of flash floods

330 will decrease, they will become more devastating.

The construction of climate models always involves a simplified presentation of real-world processes and the need for

parameterizations. To account for the uncertainties, we plan to extend this analysis in future work with an assessment based on

multiple CP-RCMs.

Author contributions.   Marjanne Zander: Methodology, Validation, Formal analysis, Investigation, Data curation, Writing - original draft,

335   Visualization.

Pety Viguurs: Methodology, Validation, Formal analysis, Investigation, Writing - review & editing.

Frederiek Sperna Weiland: Conceptualization, Methodology, Writing - review & editing, Supervision.

Albrecht Weerts: Conceptualization, Methodology, Writing - review & editing, Project administration, Funding acquisition, Supervision.

Competing interests. Prof. dr. Albrecht H. Weerts and dr. Frederiek C. Sperna Weiland are editors at HESS.

References

Alfieri, L., Burek, P., Feyen, L., and Forzieri, G.: Global warming increases the frequency of river floods in Europe, Hydrology and Earth System Sciences, 19, 2247–2260, https://doi.org/10.5194/hess-19-2247-2015, 2015.

Amponsah, W., Ayral, P.-A., Boudevillain, B., Bouvier, C., Braud, I., Brunet, P., Delrieu, G., Didon-Lescot, J.-F., Gaume, E., Lebouc, L., et al.: Integrated high-resolution dataset of high-intensity European and Mediterranean flash floods, Earth System Science Data, 10, 1783–1794, https://doi.org/10.5194/essd-10-1783-2018, 2018.

Ban, N., Schmidli, J., and Schär, C.: Evaluation of the convection-resolving regional climate modeling approach in decade-long simulations, Journal of Geophysical Research: Atmospheres, 119, 7889–7907, https://doi.org/10.1002/2014JD021478, 2014.

Ban, N., Schmidli, J., and Schär, C.: Heavy precipitation in a changing climate: Does short-term summer precipitation increase faster?, Geophysical Research Letters, 42, 1165–1172, https://doi.org/10.1002/2014GL062588, 2015.

Ban, N., Caillaud, C., Coppola, E., Pichelli, E., Sobolowski, S., Adinolfi, M., Ahrens, B., Alias, A., Anders, I., Bastin, S., Belušić, D., Berthou, S., Brisson, E., Cardoso, R. M., Chan, Steven C.and Christensen, O. B., Fernández, J., Fita, L., Frisius, T., Gašparac, G., Giorgi, F., Goergen, K., Haugen, J. E., Hodnebrog, Ø., Kartsios, S., Katragkou, E., Kendon, E. J., Keuler, K., Lavin-Gullon, A., Lenderink, G., Leutwyler, D., Lorenz, T., Maraun, D., Mercogliano, P., Milovac, J., Panitz, H.-J., Raffa, M., Remedio, A. R., Schär, C., Soares, P. M. M., Srnec, L., Steensen, B. M., Stocchi, P., Tölle, M. H., Truhetz, H., Vergara-Temprado, J., de Vries, H., Warrach-Sagi, K., Wulfmeyer, V., and Zander, M. J.: The first multi-model ensemble of regional climate simulations at kilometer-scale resolution, part I: evaluation of precipitation, Climate Dynamics, pp. 1–28, https://doi.org/https://doi.org/10.1007/s00382-021-05708-w, 2021.

Barredo, J. I.: Major flood disasters in Europe: 1950–2005, Natural Hazards, 42, 125–148, 2007.

Bell, V. A., Kay, A. L., Jones, R. G., and Moore, R. J.: Development of a high resolution grid-based river flow model for use with regional climate model output, Hydrology and Earth System Sciences, 11, 532–549, https://doi.org/10.5194/hess-11-532-2007, 2007.

Berthou, S., Kendon, E. J., Chan, S. C., Ban, N., Leutwyler, D., Schär, C., and Fosser, G.: Pan-European climate at convection-permitting scale: a model intercomparison study, Climate Dynamics, pp. 1–25, https://doi.org/10.1007/s00382-018-4114-6, 2018.

Brunner, M. I., Hingray, B., Zappa, M., and Favre, A.-C.: Future Trends in the Interdependence Between Flood Peaks and Volumes: Hydro-Climatological Drivers and Uncertainty, Water Resources Research, 55, 4745–4759, https://doi.org/https://doi.org/10.1029/2019WR024701, 2019.

Bundesamt für Umwelt: Hydrological Data Service for watercourses and lakes, https://www.bafu.admin.ch/bafu/en/home/topics/water/state/data/obtaining-monitoring-data-on-the-topic-of-water/hydrological-data-service-for-watercourses-and-lakes.html, 2021.

Cloke, H. L., Wetterhall, F., He, Y., Freer, J. E., and Pappenberger, F.: Modelling climate impact on floods with ensemble climate projections, Quarterly Journal of the Royal Meteorological Society, 139, 282–297, 2013.

Coppola, E., Stefan, S., Pichelli, E., Raffaele, F., Ahrens, B., Anders, I., Ban, N., Bastin, S., Belda, M., Belusic, D., Caldas-Alvarez, A., Cardoso, R. M., Davolio, S., Dobler, A., Fernandez, J., Fita, L., Fumiere, Q., Giorgi, F., Goergen, K., Güttler, I., Halenka, T., Heinzeller, D., Hodnebrog, O., Jacob, D., Kartsios, S., Katragkou, E., Kendon, E., Khodayar, S., Kunstmann, H., Knist, S., Lavín-Gullón, A., Lind, P., Lorenz, T., Maraun, D., Marelle, L., van Meijgaard, E., Milovac, J., Myhre, G., H-J, P., Piazza, M., Raffa, M., Raub, T., Rockel, B., Schär, C., Sieck, K., Soares, P. M. M., Somot, S., Srnec, L., Stocchi, P., Tölle, M., Truhetz, H., Vautard, R., de Vries, H., and Warrach-Sagi, K.: A first-of-its-kind multi-model convection permitting ensemble for investigating convective phenomena over Europe and the Mediterranean, Climate Dynamics, 55, 3–34, https://search-proquest-com.ezproxy.library.wur.

nl/scholarly-journals/first-kind-multi-model-convection-permitting/docview/2132129428/se-2?accountid=27871, copyright - Springer-Verlag GmbH Germany, part of Springer Nature 2018; Last updated - 2020-06-27; SubjectsTermNotLitGenreText - Alps; Europe, 2020.

de Bruin, H. A. R., Trigo, I. F., Bosveld, F. C., and Meirink, J. F.: A Thermodynamically Based Model for Actual Evapotranspiration of an Extensive Grass Field Close to FAO Reference, Suitable for Remote Sensing Application, Journal of Hydrometeorology, 17, 1373 – 1382,
385   https://doi.org/10.1175/JHM-D-15-0006.1, 2016.

Dee, D. P., Uppala, S. M., Simmons, A. J., Berrisford, P., Poli, P., Kobayashi, S., Andrae, U., Balmaseda, M. A., Balsamo, G., Bauer, P., Bechtold, P., Beljaars, A. C. M., van de Berg, L., Bidlot, J., Bormann, N., Delsol, C., Dragani, R., Fuentes, M., Geer, A. J., Haimberger, L., Healy, S. B., Hersbach, H., Holm, E. V., Isaksen, L., Kallberg, P., Koehler, M., Matricardi, M., McNally, A. P., Monge-Sanz, B. M., Morcrette, J., Park, B., Peubey, C., de Rosnay, P., Tavolato, C., Thepaut, J., and Vitart, F.: The ERA-Interim reanalysis:
390   configuration and performance of the data assimilation system, Quarterly Journal of the Royal Meteorological Society, 137, 553–597, https://doi.org/10.1002/qj.828, 2011.

Di Sante, F., Coppola, E., and Giorgi, F.: Projections of river floods in Europe using EURO-CORDEX, CMIP5 and CMIP6 simulations, International Journal of Climatology, 41, 3203–3221, https://doi.org/https://doi.org/10.1002/joc.7014, 2021.

Dipartimento Protezione Civile, Provincia Autonoma di Trento, Trento: Dati Storici, https://www.floods.it/public/DatiStorici.php, 2019.

395   Doswell, C. A., Brooks, H. E., and Maddox, R. A.: Flash Flood Forecasting: An Ingredients-Based Methodology, Weather and Forecasting, 11, 560 – 581, https://doi.org/10.1175/1520-0434(1996)011<0560:FFFAIB>2.0.CO;2, 1996.

Eilander, D., van Verseveld, W., Yamazaki, D., Weerts, A., Winsemius, H. C., and Ward, P. J.: A hydrography upscaling method for scale-invariant parametrization of distributed hydrological models, Hydrology and Earth System Sciences, 25, 5287–5313, https://doi.org/10.5194/hess-25-5287-2021, 2021.

400   Eilander, D., Boisgontier, H., e. Bouaziz, L. J., Buitink, J., Couasnon, A., Dalmijn, B., Hegnauer, M., de Jong, T., Loos, S., Marth, I., and van Verseveld, W.: HydroMT: Automated and reproducible model building and analysis, Journal of Open Source Software, 8, 4897, https://doi.org/10.21105/joss.04897, 2023.

Felder, G., Gómez-Navarro, J. J., Zischg, A. P., Raible, C. C., Röthlisberger, V., Bozhinova, D., Martius, O., and Weingartner, R.: From global circulation to local flood loss: Coupling models across the scales, Science of The Total Environment, 635, 1225 – 1239,
405   https://doi.org/https://doi.org/10.1016/j.scitotenv.2018.04.170, 2018.

Förster, K. and Thiele, L.-B.: Variations in sub-daily precipitation at centennial scale, npj Climate and Atmospheric Science, 3, 1–7, https://doi.org/10.1038/s41612-020-0117-1, 2020.

Fosser, G., Khodayar, S., and Berg, P.: Climate change in the next 30 years: What can a convection-permitting model tell us that we did not already know?, Climate Dynamics, 48, 1987–2003, https://doi.org/https://doi.org/10.1007/s00382-016-3186-4, 2017.

410   Froidevaux, P., Schwanbeck, J., Weingartner, R., Chevalier, C., and Martius, O.: Flood triggering in Switzerland: the role of daily to monthly preceding precipitation, Hydrology and Earth System Sciences, 19, 3903–3924, https://doi.org/10.5194/hess-19-3903-2015, 2015.

Fumière, Q., Déqué, M., Nuissier, O., Somot, S., Alias, A., Caillaud, C., Laurantin, O., and Seity, Y.: Extreme rainfall in Mediterranean France during the fall: added value of the CNRM-AROME Convection-Permitting Regional Climate Model, Climate Dynamics, 55, 77–91, 2020.

415   Gaume, E., Bain, V., Bernardara, P., Newinger, O., Barbuc, M., Bateman, A., Blaškovičová, L., Blöschl, G., Borga, M., Dumitrescu, A., et al.: A compilation of data on European flash floods, Journal of Hydrology, 367, 70–78, https://doi.org/10.1016/j.jhydrol.2008.12.028, 2009.

Global Land Ice Measurements from Space (GLIMS): Randolph Glacier Inventory (RGI) - A Dataset of Global Glacier Outlines: Version 6.0: Technical Report, https://doi.org/https://doi.org/10.7265/N5-RGI-60, 2017.

Global Runoff Data Centre : GRDC Data Portal, https://portal.grdc.bafg.de/applications/public.html?publicuser=PublicUser#dataDownload/
420   Home, 2021.

Gobiet, A., Kotlarski, S., Beniston, M., Heinrich, G., Rajczak, J., and Stoffel, M.: 21st century climate change in the European Alps - a
         review, Science of the Total Environment, 493, 1138–1151, https://doi.org/https://doi.org/10.1016/j.scitotenv.2013.07.050, 2014.

Gupta, H. V., Kling, H., Yilmaz, K. K., and Martinez, G. F.: Decomposition of the mean squared error and NSE performance criteria:
         Implications for improving hydrological modelling, Journal of hydrology, 377, 80–91, 2009.

425   Hagemann, S., Chen, C., Haerter, J. O., Heinke, J., Gerten, D., and Piani, C.: Impact of a statistical bias correction on the projected hydro-
         logical changes obtained from three GCMs and two hydrology models, Journal of Hydrometeorology, 12, 556–578, 2011.

Hazeleger, W., Van Den Hurk, B. J. J. M., Min, E., Van Oldenborgh, G. J., Petersen, A. C., Stainforth, D. A., Vasileiadou, E., and Smith,
         L. A.: Tales of future weather, Nature Climate Change, 5, 107–113, www.scopus.com, cited By :14, 2015.

Hegdahl, T. J., Engeland, K., Müller, M., and Sillmann, J.: An Event-Based Approach to Explore Selected Present and Future Atmospheric
430   River–Induced Floods in Western Norway, Journal of Hydrometeorology, 21, 2003 – 2021, https://doi.org/10.1175/JHM-D-19-0071.1,
         2020.

Hersbach, H., de Rosnay, P., Bell, B., Schepers, D., Simmons, A., Soci, C., Abdalla, S., Alonso-Balmaseda, M., Balsamo, G., Bechtold, P.,
         Berrisford, P., Bidlot, J.-R., de Boisséson, E., Bonavita, M., Browne, P., Buizza, R., Dahlgren, P., Dee, D., Dragani, R., Diamantakis, M.,
         Flemming, J., Forbes, R., Geer, A. J., Haiden, T., Hólm, E., Haimberger, L., Hogan, R., Horányi, A., Janiskova, M., Laloyaux, P., Lopez,
435   P., Munoz-Sabater, J., Peubey, C., Radu, R., Richardson, D., Thépaut, J.-N., Vitart, F., Yang, X., Zsótér, E., and Zuo, H.: Operational
         global reanalysis: progress, future directions and synergies with NWP, ERA Report Series, https://doi.org/10.21957/tkic6g3wm, 2018.

Imhoff, R., van Verseveld, W., van Osnabrugge, B., and Weerts, A.: Scaling Point-Scale (Pedo)transfer Functions to Seamless Large-Domain
         Parameter Estimates for High-Resolution Distributed Hydrologic Modeling: An Example for the Rhine River, Water Resources Research,
         56, https://doi.org/10.1029/2019WR026807, 2020.

440   Jacob, D., Petersen, J., Eggert, B., Alias, A., Christensen, O. B., Bouwer, L. M., Braun, A., Colette, A., Déqué, M., Georgievski, G., et al.:
         EURO-CORDEX: new high-resolution climate change projections for European impact research, Regional environmental change, 14,
         563–578, https://doi.org/10.1007/s10113-013-0499-2, 2014.

Jonkman, S. N.: Global perspectives on loss of human life caused by floods, Natural hazards, 34, 151–175, 2005.

Kay, A., Rudd, A., Davies, H., Kendon, E., and Jones, R.: Use of very high resolution climate model data for hydrological modelling: baseline
445   performance and future flood changes, Climatic Change, 133, 193–208, https://doi.org/10.1007/s10584-015-1455-6, 2015.

Kendon, E. J., Ban, N., Roberts, N. M., Fowler, H. J., Roberts, M. J., Chan, S. C., Evans, J. P., Fosser, G., and Wilkinson, J. M.: Do Convection-
         Permitting Regional Climate Models Improve Projections of Future Precipitation Change?, Bulletin of the American Meteorological
         Society, 98, 79–93, https://doi.org/10.1175/BAMS-D-15-0004.1, 2017.

Klingler, C., Kratzert, F., Schulz, K., and Herrnegger, M.: LamaH-CE: LArge-SaMple DAta for Hydrology and Environmental Sciences for
450   Central Europe - files, https://doi.org/10.5281/zenodo.5153305, 2021.

Kuksina, L., Golosov, V., and Kuznetsova, Y. S.: Cloudburst floods in mountains: State of knowledge, occurrence, factors of formation,
         Geography and Natural Resources, 38, 20–29, https://doi.org/10.1134/S1875372817010036, 2017.

Lavin-Gullon, A., Fernandez, J., Bastin, S., Cardoso, R. M., Fita, L., Giannaros, T. M., Goergen, K., Gutierrez, J. M., Kartsios, S., Katragkou,
         E., Lorenz, T., Milovac, J., Soares, P. M. M., Sobolowski, S., and Warrach-Sagi, K.: Internal variability versus multi-physics uncertainty
455   in a regional climate model, International Journal of Climatology, 41, E656–E671, https://doi.org/https://doi.org/10.1002/joc.6717, 2021.

Hydrology and
Earth System
Sciences
Discussions

Lehner, B., Liermann, C. R., Revenga, C., Vörösmarty, C., Fekete, B., Crouzet, P., Döll, P., Endejan, M., Frenken, K., Magome, J., et al.: Global reservoir and dam (grand) database, Technical Documentation, Version, 1, 1–14, 2011.

Lenderink, G. and Van Meijgaard, E.: Increase in hourly precipitation extremes beyond expectations from temperature changes, Nature Geoscience, 1, 511–514, 2008.

460 Lenderink, G. and Van Meijgaard, E.: Linking increases in hourly precipitation extremes to atmospheric temperature and moisture changes, Environmental Research Letters, 5, 025 208, 2010.

Leutwyler, D., Lüthi, D., Ban, N., Fuhrer, O., and Schär, C.: Evaluation of the convection-resolving climate modeling approach on continental scales, Journal of Geophysical Research: Atmospheres, 122, 5237–5258, https://doi.org/10.1002/2016JD026013, 2017.

Li, J., Evans, J., Johnson, F., and Sharma, A.: A comparison of methods for estimating climate change impact on design rainfall using a
465 high-resolution RCM, Journal of Hydrology, 547, 413 – 427, https://doi.org/https://doi.org/10.1016/j.jhydrol.2017.02.019, 2017.

Lucas-Picher, P., Argüeso, D., Brisson, E., Tramblay, Y., Berg, P., Lemonsu, A., Kotlarski, S., and Caillaud, C.: Convection-permitting modeling with regional climate models: Latest developments and next steps, WIREs Climate Change, n/a, e731, https://doi.org/https://doi.org/10.1002/wcc.731, 2021.

Manola, I., van den Hurk, B., De Moel, H., and Aerts, J.: Future extreme precipitation intensities based on historic events, Hydrology and
470 Earth System Sciences Discussions, https://doi.org/https://doi.org/10.5194/hess-2017-227, under review, 2017.

Marani, M. and Ignaccolo, M.: A metastatistical approach to rainfall extremes, Advances in Water Resources, 79, 121 – 126, https://doi.org/https://doi.org/10.1016/j.advwatres.2015.03.001, 2015.

Marchi, L., Borga, M., Preciso, E., and Gaume, E.: Characterisation of selected extreme flash floods in Europe and implications for flood risk management, Journal of Hydrology, 394, 118–133, https://doi.org/https://doi.org/10.1016/j.jhydrol.2010.07.017, flash Floods: Obser-
475 vations and Analysis of Hydrometeorological Controls, 2010.

Marra, F., Nikolopoulos, E. I., Anagnostou, E. N., and Morin, E.: Metastatistical Extreme Value analysis of hourly rainfall from short records: Estimation of high quantiles and impact of measurement errors, Advances in Water Resources, 117, 27–39, https://doi.org/https://doi.org/10.1016/j.advwatres.2018.05.001, 2018.

Meile, T., Boillat, J.-L., and Schleiss, A.: Hydropeaking indicators for characterization of the Upper-Rhone River in Switzerland, Aquatic
480 Sciences, 73, 171–182, https://doi.org/10.1007/s00027-010-0154-7, 2011.

Messager, M. L., Lehner, B., Grill, G., Nedeva, I., and Schmitt, O.: Estimating the volume and age of water stored in global lakes using a geo-statistical approach, Nature communications, 7, 1–11, 2016.

Modrick, T. M. and Georgakakos, K. P.: The character and causes of flash flood occurrence changes in mountainous small basins of Southern California under projected climatic change, Journal of Hydrology: Regional Studies, 3, 312–336, 2015.

485 Myneni, R. B., Knyazikhin, Y., and Park, T.: MCD15A3H MODIS/Terra+Aqua Leaf Area Index/FPAR 4-day L4 Global 500m SIN Grid V006 (Tech. Rep.), NASA EOSDIS and Pocesses DAAC, 2015.

Nogueira, M.: Inter-comparison of ERA-5, ERA-interim and GPCP rainfall over the last 40 years: Process-based analysis of systematic and random differences, Journal of Hydrology, 583, 124 632, https://doi.org/https://doi.org/10.1016/j.jhydrol.2020.124632, 2020.

OpenStreetMap contributors: Planet dump retrieved from https://planet.osm.org , https://www.openstreetmap.org, 2017.

490 Paprotny, D., Morales Napoles, O., and Jonkman, S. N.: HANZE database of historical damaging floods in Europe, 1870-2016., https://doi.org/10.4121/uuid:5b75be6a-4dd4-472e-9424-f7ac4f7367f6, 2017.

Pichelli, E., Coppola, E., Sobolowski, S., Ban, N., Giorgi, F., Stocchi, P., Alias, A., Belušić, D., Berthou, S., Caillaud, C., Cardoso, R. M., Chan, S., Christensen, O. B., Dobler, A., de Vries, H., Goergen, K., Kendon, E. J., Keuler, K., Lenderink, G., Lorenz, T., Mishra, A. N.,

Hydrology and
Earth System
Sciences
Discussions

Open Access
EGU

Panitz, H.-J., Schär, C., Soares, P. M. M., Truhetz, H., and Vergara-Temprado, J.: The first multi-model ensemble of regional climate simulations at kilometer-scale resolution part 2: historical and future simulations of precipitation, Climate Dynamics, 56, 3581–3602, https://doi.org/10.1007/s00382-021-05657-4, 2021.

Prein, A. F., Gobiet, A., Suklitsch, M., Truhetz, H., Awan, N. K., Keuler, K., and Georgievski, G.: Added value of convection permitting seasonal simulations, Climate Dynamics, 41, 2655–2677, https://doi.org/10.1007/s00382-013-1744-6, 2013.

Prein, A. F., Langhans, W., Fosser, G., Ferrone, A., Ban, N., Goergen, K., Keller, M., Tölle, M., Gutjahr, O., Feser, F., Brisson, E., Kollet, S., Schmidli, J., van Lipzig, N. P. M., and Leung, R.: A review on regional convection-permitting climate modeling: Demonstrations, prospects, and challenges, Reviews of Geophysics, 53, 323–361, https://doi.org/10.1002/2014RG000475, 2014RG000475, 2015.

Quaile, E. L.: Back to basics: Foehn and chinook winds, Weather, 56, 141–145, https://doi.org/10.1002/j.1477-8696.2001.tb06551.x, 2001.

Reszler, C., Switanek, M. B., and Truhetz, H.: Convection-permitting regional climate simulations for representing floods in small- and medium-sized catchments in the Eastern Alps, Natural Hazards and Earth System Sciences, 18, 2653–2674, https://doi.org/10.5194/nhess-18-2653-2018, 2018.

Rudd, A. C., Kay, A. L., Wells, S. C., Aldridge, T., Cole, S. J., Kendon, E. J., and Stewart, E. J.: Investigating potential future changes in surface water flooding hazard and impact, Hydrological Processes, 34, 139–149, https://doi.org/10.1002/hyp.13572, 2020.

Schaller, N., Sillmann, J., Müller, M., Haarsma, R., Hazeleger, W., Hegdahl, T. J., Kelder, T., van den Oord, G., Weerts, A., and Whan, K.: The role of spatial and temporal model resolution in a flood event storyline approach in western Norway, Weather and Climate Extremes, 29, 100 259, https://doi.org/https://doi.org/10.1016/j.wace.2020.100259, 2020.

Schär, C., Davies, T. D., Frei, C., Wanner, H., Widmann, M., Wild, M., and Davies, H. C.: Current alpine climate, The MIT Press, 1998.

Schellekens, J., Van Verseveld, W., Visser, M., Winsemius, H., Euser, T., Bouaziz, L., Boisgontier, H., et al.: Openstreams/wflow: Unstable-master, https://github.com/openstreams/wflow, 2021.

Smiatek, G. and Kunstmann, H.: Simulating Future Runoff in a Complex Terrain Alpine Catchment with EURO-CORDEX Data, Journal of Hydrometeorology, 20, 1925 – 1940, https://doi.org/10.1175/JHM-D-18-0214.1, 2019.

Sperna Weiland, F. C., Visser, R. D., Greve, P., Bisselink, B., Brunner, L., and Weerts, A. H.: Estimating Regionalized Hydrological Impacts of Climate Change Over Europe by Performance-Based Weighting of CORDEX Projections, Frontiers in Water, 3, https://doi.org/10.3389/frwa.2021.713537, 2021.

Tarolli, P., Borga, M., Morin, E., and Delrieu, G.: Analysis of flash flood regimes in the North-Western and South-Eastern Mediterranean regions, Natural Hazards and Earth System Sciences, 12, 1255–1265, https://doi.org/10.5194/nhess-12-1255-2012, 2012.

Themeßl, M. J., Gobiet, A., and Heinrich, G.: Empirical-statistical downscaling and error correction of regional climate models and its impact on the climate change signal, Climatic Change, 112, 449–468, 2012.

van Osnabrugge, B., Uijlenhoet, R., and Weerts, A.: Contribution of potential evaporation forecasts to 10-day streamflow forecast skill for the Rhine River, Hydrology and Earth System Sciences, 23, 1453–1467, https://doi.org/10.5194/hess-23-1453-2019, 2019.

van Verseveld, W. J., Weerts, A. H., Visser, M., Buitink, J., Imhoff, R. O., Boisgontier, H., Bouaziz, L., Eilander, D., Hegnauer, M., ten Velden, C., and Russell, B.: Wflow_sbm v0.6.1, a spatially distributed hydrologic model: from global data to local applications, Geoscientific Model Development Discussions, 2022, 1–52, https://doi.org/10.5194/gmd-2022-182, 2022.

van Vuuren, D. P., Edmonds, J., Kainuma, M., Riahi, K., Thomson, A., Hibbard, K., Hurtt, G. C., Kram, T., Krey, V., Lamarque, J.-F., Masui, T., Meinshausen, M., Nakicenovic, N., Smith, S. J., and Rose, S. K.: The representative concentration pathways: an overview, Climatic Change, 109, 5, https://doi.org/10.1007/s10584-011-0148-z, 2011.

Westra, S., Fowler, H. J., Evans, J. P., Alexander, L. V., Berg, P., Johnson, F., Kendon, E. J., Lenderink, G., and Roberts, N. M.: Future changes to the intensity and frequency of short-duration extreme rainfall, Reviews of Geophysics, 52, 522–555, https://doi.org/10.1002/2014RG000464, 2014.

Williams, K. D., Copsey, D., Blockley, E. W., Bodas-Salcedo, A., Calvert, D., Comer, R., Davis, P., Graham, T., Hewitt, H. T., Hill, R., Hyder,
535   P., Ineson, S., Johns, T. C., Keen, A. B., Lee, R. W., Megann, A., Milton, S. F., Rae, J. G. L., Roberts, M. J., Scaife, A. A., Schiemann, R., Storkey, D., Thorpe, L., Watterson, I. G., Walters, D. N., West, A., Wood, R. A., Woollings, T., and Xavier, P. K.: The Met Office Global Coupled Model 3.0 and 3.1 (GC3.0 and GC3.1) Configurations, Journal of Advances in Modeling Earth Systems, 10, 357–380, https://doi.org/10.1002/2017MS001115, 2018.

Yamazaki, D., Ikeshima, D., Sosa, J., Bates, P. D., Allen, G. H., and Pavelsky, T. M.: MERIT Hydro: A High-
540   Resolution Global Hydrography Map Based on Latest Topography Dataset, Water Resources Research, 55, 5053–5073, https://doi.org/https://doi.org/10.1029/2019WR024873, 2019.

Zekollari, H., Huss, M., and Farinotti, D.: Modelling the future evolution of glaciers in the European Alps under the EURO-CORDEX RCM ensemble, The Cryosphere, 13, 1125–1146, https://doi.org/10.5194/tc-13-1125-2019, 2019.

Zorzetto, E., Botter, G., and Marani, M.: On the emergence of rainfall extremes from ordinary events, Geophysical Research Letters, 43,
545   8076–8082, https://doi.org/10.1002/2016GL069445, 2016.

Appendix A: Hydrological model parameter sensitivity analysis

Table A1. Sensitivity analysis of Horizontal Saturated Hydraulic Conductivity as a factor of the Vertical Saturated Hydraulic Conductivity (KsatHor) for discharge at the Rhine river at Basel and the Thur river at Andelfingen.

| Parameter | Rhine basin submodel (2002-01-01 - 2010-12-31) - Mean Daily Discharge | | | | | | | | | | | |
| | Basel | | | | | | Thur - Andelfingen | | | | | |
KsatHor	5	20	50	100	200	500	5	20	50	100	200	500
RMSE	299.47	303.34	291.79	277.67	264.79	257.72	45.63	42.09	37.94	34.40	31.94	32.07
NSE	0.47	0.45	0.49	0.54	0.58	0.61	0.13	0.26	0.40	0.51	0.57	0.57
KGE	0.74	0.73	0.73	0.72	0.69	0.63	0.61	0.65	0.70	0.75	0.75	0.58
cc	0.75	0.73	0.74	0.75	0.77	0.79	0.77	0.77	0.77	0.78	0.78	0.76
alpha	0.94	0.99	1.05	1.12	1.20	1.30	0.69	0.74	0.82	0.93	1.08	1.33
beta	0.99	0.98	0.97	0.96	0.96	0.95	0.93	0.93	0.92	0.92	0.91	0.90

Appendix B: Sensitivity of model results to end-of-century glacier retreat for the Rhone basin submodel
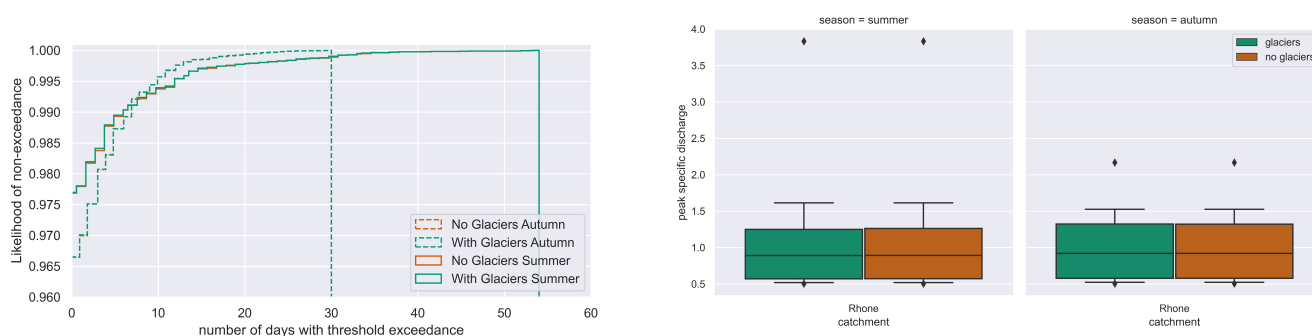
(a) Threshold exceedance cummulative frequency distribution, same methodology as figure 6

(b) Threshold exceedance magnitudes, same methodology as figure 7

Figure A1. Comparison Future Climate simulation for summer (JJA) and autumn (SON) for the Rhone with initialised glacier extents and volumes ('glaciers', green) and without glaciers to reflect a scenario with complete glacier retreat for the end-of-century ('no glaciers', orange).